Detailed Active Site Configuration of a New Crystal Form of Methanol Dehydrogenase from *Methylophilus* W3A1 at 1.9 Å Resolution[†,‡]

Zong-xiang Xia,[§] Yong-ning He,[§,||] Wei-wen Dai,[§,||] Scott A. White,[||,⊥] Geoffrey D. Boyd,[||] and F. Scott Mathews*[,||]

Shanghai Institute of Organic Chemistry, Chinese Academy of Sciences, Shanghai 200032, China, and Department of Biochemistry and Molecular Biophysics, Washington University School of Medicine, St. Louis, Missouri 63110

Received September 18, 1998; Revised Manuscript Received November 18, 1998

ABSTRACT: The three-dimensional structure of a new crystal form of methanol dehydrogenase from *Methylophilus* W3A1 has been obtained in the presence of substrate using data recorded at a synchrotron. The structure of this ~140 kDa heterotetramer, refined at 1.9 Å resolution, reveals the detailed configuration of its redox cofactor, pyrroloquinoline quinone (PQQ). C4, one of the oxygen-bearing atoms of this orthoquinone is in a planar configuration while C5, which bears the other quinone oxygen, is tetrahedral, suggesting that the PQQ is in the semiquinone redox state. The substrate binding site has been identified close to PQQ and to the side chain of Asp297, the putative active site base. The proximity of the hydroxyl of methanol to C5 of PQQ compared to the greater separation of the substrate methyl group from C5 supports the addition−elimination reaction mechanism involving a hemiketal intermediate.

Methanol dehydrogenase (MEDH,[1] EC 1.1.99.8) is a periplasmic quinoprotein of approximate molecular mass of 140 kDa that is isolated from certain methylotrophic bacteria. It catalyzes the oxidation of methanol or of other primary alcohols to the corresponding aldehyde with the release of two protons and two electrons. The physiological electron acceptor from MEDH is the acidic cytochrome c_L (*1*). The electrons are subsequently delivered to the cytochrome a/a_3 complex of the periplasmic membrane.

MEDH is an H_2L_2 heterotetramer. In the case of *Methylophilus* W3A1, each of the heavy (H) and light (L) subunits consists of 571 and 69 amino acid residues, respectively (*2*). Each H subunit contains one molecule of the prosthetic group pyrroloquinolinequinone (PQQ) (Figure 1) which is noncovalently bound to the polypeptide chain (*3*), as well as one calcium ion which is essential for its enzymatic function (*4*).

The three-dimensional structures of MEDH from two methylotrophic bacteria, *Methylophilus methylotrophus* and *Methylophilus* W3A1, were determined at 2.6 Å resolution (*5*) and were the first reported structures of a PQQ-containing enzyme. The active site structure (*6*), the gene sequence, and the complete structure of MEDH from *M.* W3A1 (crystal form *A*) refined at 2.4 Å resolution (*2*), as well as the three-dimensional structure of MEDH from *Methylobacterium extorquens* AM1 determined at 1.94 Å resolution (*7*), have been reported.

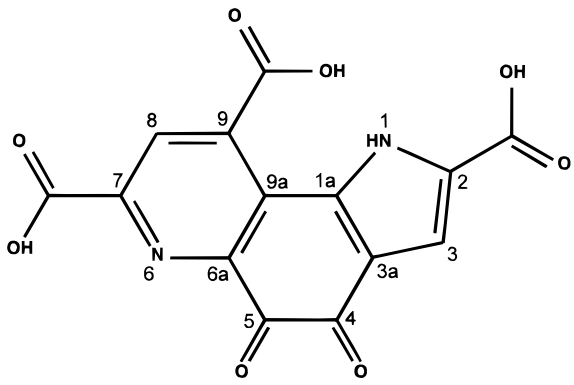

FIGURE 1: Chemical structure of PQQ.

We have grown single crystals of MEDH from *M.* W3A1 in a new crystal form (form *B*) and determined its structure in the presence of methanol by the molecular replacement method (*8*). In this paper we present the three-dimensional structure of the new crystal form, refined at high resolution (1.9 Å), which provides information on the detailed configuration of the prosthetic group and the substrate binding site, and helps elucidate the mechanism of the enzymatic reaction.

EXPERIMENTAL PROCEDURES

Enzyme Purification and Crystal Growth. Methanol dehydrogenase was isolated from *M.* W3A1 according to published procedures (*9*). Form *B* crystals of MEDH from *M.* W3A1 were grown by directly mixing the protein with the precipitant and buffer. The crystallization solution contained 3 mg/mL MEDH, 10% PEG8000, 50 mM tris-HCl, pH 8.25, and 4 mM methanol. The crystals belong to space group $\bar{P}2_1$ with cell parameters $a = 98.1$ Å, $b = 69.7$ Å, $c = 109.8$ Å, and $\beta = 110.25°$. For comparison, the cell dimensions of the form *A* crystals, also in space group $\bar{P}2_1$, are $a = 124.7$ Å, $b = 62.9$ Å, $c = 85.0$ Å, and $\beta = 93.6°$. The crystallization conditions for form *A* differ from those

[†] This work was supported by grants from Chinese Academy of Sciences, the National Natural Science Foundation of China and by USPHS Grant No. GM31611.

[‡] Crystallographic coordinates have been deposited in the Brookhaven Protein Data Bank under the file name 1B2N.

* Corresponding Author. Tel: 314-362-1080. Fax: 314-362-7183. E-mail: mathews@biochem.wustl.edu.

[§] Chinese Academy of Sciences.

[||] Washington University School of Medicine.

[⊥] Present Address: School of Biochemistry, University of Birmingham, Birmingham B15 2TT England.

[1] Abbreviations: MEDH, methanol dehydrogenase; PQQ, pyrroloquinolinequinone; rms, root-mean-square.

10.1021/bi9822574 CCC: $18.00
Published on Web 12/31/1998

Table 1: Area Detector X-ray Data Collection Statistics

shell lower limit (Å)	no. of reflections possible	no. of reflections collected	no. of observations	R_{sym}[a] (%)	$\langle I/\sigma(I)\rangle$[b]
3.52	17 569	17 426	149 433	5.6	39.6
2.79	17 336	17 246	111 543	12.5	11.7
2.44	17 239	16 979	75 486	22.3	4.6
2.22	17 256	16 050	37 047	27.6	2.0
2.06	16 843	10 874	17 943	30.3	1.4
total	86 243	78 575	391 452	9.2	13.0

[a] $R_{sym} = \sum|I - \langle I\rangle|/\sum I$. [b] Signal-to-noise ratio for merged reflections.

Table 2: Synchrotron X-ray Data Collection Statistics

crystal code	radius of cassette (mm)	Weisenberg Strategy spindle	rotation of each IP (deg)	total rotation range (deg)	dmin (Å)
1	286.5	b	7.0	195.5	1.8
2	286.5	a	3.5	60.5	2.1

shell lower limit (Å)	Data Collection Statistics[a] no. of reflections	completeness (%)	R_{sym}[b] (%)	$\langle I/\sigma(I)\rangle$[c]
4.09[d]	11 114	99.0	3.6	34.3
3.25	11 062	100.0	4.7	26.3
2.84	10 994	100.0	7.7	17.4
2.58	10 960	100.0	12.1	11.7
2.39	10 952	99.9	17.1	8.7
2.25	10 848	99.1	22.3	6.9
2.14	10 744	98.2	29.8	5.2
2.05	10 636	97.6	40.6	3.7
1.97	10 585	96.8	55.9	2.7
1.90	10 453	95.6	81.3	1.9
total	108 348	98.6	9.1	15.5

[a] All data with $I > -3\sigma(I)$ were included in the scaling. [b] $R_{sym} = \sum|I - \langle I\rangle|/\sum\langle I\rangle$. [c] Signal-to-noise ratio for merged reflections. [d] 40.0−4.09 Å.

of form *B* mainly in the higher PEG8000 concentration (13%) (*5, 10*). Assuming there is one heterotetrameric molecule in an asymmetric unit, the volume per unit protein molecular mass, V_M (*11*) is 2.50 Å^3/Da, slightly higher than that of form *A* crystals (V_M = 2.36 Å^3/Da).

Data Collection. Two kinds of X-ray data were collected. (1) Multiwire (ADSC, Poway, CA) area detector data were collected from two crystals that were mounted in a mother liquor-filled X-ray capillary and immobilized by cotton fibers. The data were processed using software developed at the University of California at San Diego (*12*) and were 99% complete to 2.4 Å resolution. (2) Synchrotron data (National Laboratory for High Energy Physics, Tsukuba, Japan) were collected from two crystals that were mounted in sealed X-ray capillaries without additional mother liquor. The data were recorded at 4 °C using Weissenberg cassettes fitted with image plates (*13*); the two crystals were aligned, one with the *a* axis and one with the *b* axis approximately parallel to the spindle, respectively. The data were processed using DENZO (*14*). Although the multiwire and the synchrotron data were recorded to limits of 2.06 and 1.80 Å, respectively, the signal-to-noise ratio ($I/\sigma(I)$) was too low at those limits and structural refinement was restricted to 2.4 and 1.9 Å, respectively. The data collection statistics for the multiwire and synchrotron data are shown in Tables 1 and 2, respectively.

Structure Analysis and Refinement. The structure of the form *B* MEDH crystals was determined using the multiwire data by the molecular replacement method using the program package MERLOT (*15*). The structure of the form *A* crystals, refined at 2.4 Å resolution, was used as the search model, but with PQQ, Ca^{2+}, and all of the water molecules omitted and the temperature factors of all the atoms set to 15.0 Å^2. Data were limited to $I > 3\sigma(I)$ within the resolution range of 8−4 Å. The Crowther fast rotation function (*16*) was applied first, followed by analysis of the Lattman and Love rotation function (*17*) and the Crowther and Blow translation function (*18*). The single prominent molecular replacement solution that resulted was then subjected to a rigid body *R*-factor minimization procedure and gave an *R*-factor of 0.325 after scale factor refinement using the program PROLSQ (*19*).

Crystallographic refinement was carried out using the program package X-PLOR (*20*) on an INDIGO2 XZ workstation (Silicon Graphics, Mountain View, CA). Manual rebuilding was done using the TURBO−FRODO graphics software (*21*).

RESULTS

Model Refinement. Refinement of form *B* of MEDH from *M.* W3A1 was carried out in two stages. In the first stage, the multiwire data were used to refine the model at 2.4 Å resolution. Initial rigid body refinement, followed by alternate positional and temperature factor refinement, without manual model rebuilding or added water, led to an *R*-factor of 0.207 where $R = \sum_{hkl}|F_o - F_c|_{hkl}/\sum|F_o|_{hkl}$ and F_o and F_c are the observed and calculated structure factors for each reflection hkl, respectively, and the summation is over all of the reflections. An electron density difference Fourier map, computed using $(F_o - F_c)_{hkl}$ as coefficients and phases computed from the model, clearly showed electron density at the active site in each H subunit that could be matched with PQQ. After fitting PQQ and Ca^{2+} to the density, further refinement reduced the *R*-factor to 0.195. The resulting ($F_o - F_c$) difference electron density map contoured at $\pm 3.0\sigma$, where σ is the rms (root-mean-square) value of the density, showed many spherical features of positive density representing water molecules.

Near the O5 atom of PQQ in subunit H1 there was a feature of positive ($F_o - F_c$) difference electron density (contoured at $+3\sigma$) which was elongated in shape stretching upward[2] in a direction roughly perpendicular to the PQQ ring plane, as shown in Figure 2a. A weaker, elongated piece of positive electron density ($\sim 2.5\sigma$) was also found at this site in subunit H2. This density could be interpreted as methanol with its hydroxyl group near both PQQ-O5 and a carboxylate oxygen of Asp297 and the methyl group in a hydrophobic environment consisting of side chains of two tryptophans, a leucine, and a cystine disulfide.[3] Further refinement following the fitting of methanol at this site, but with no water molecules or model rebuilding, led to an *R*-factor of 0.186, with rms deviations from various ideal geometric parameters as shown in Table 3. The methanol in

[2] All descriptions of direction (upward and downward) are with respect to the preferred orientation of PQQ shown in Figure 2.

[3] The reverse orientation for methanol, with the methyl group close to the carboxylate of Asp297 and the hydroxyl group pointing into a hydrophobic pocket, would also fit the electron density, but is less likely on the basis of chemical considerations.

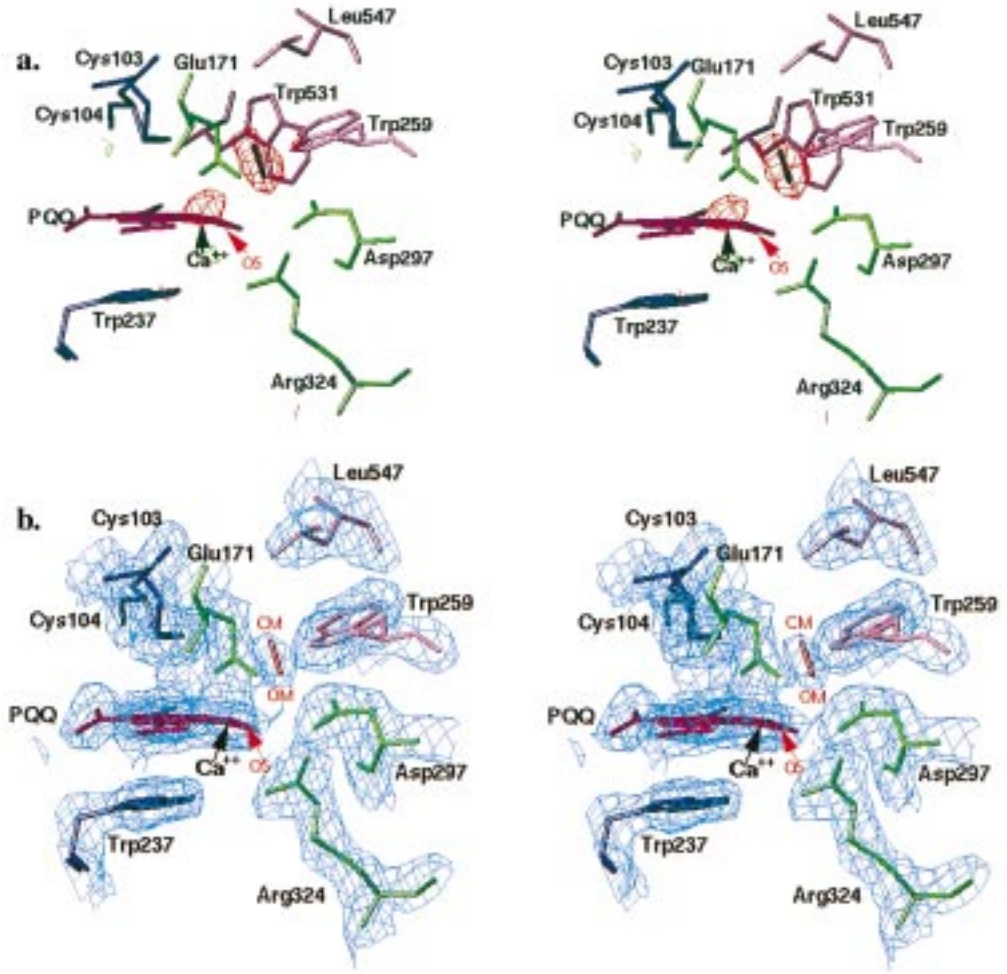

FIGURE 2: Electron density showing the substrate binding site in subunit H1, computed using multiwire data at 2.4 Å resolution and based on a model with planar PQQ restraints. The surroundings of the substrate binding site are also shown. (a) ($F_o - F_c$) difference electron density map contoured at $\pm 3.0\sigma$ ($+3.0\sigma$ in red, -3.0σ in green), computed from a model in which substrate is not included. The black bond represents a diatomic molecule not present in the model. (b) ($2F_o - F_c$) electron density map contoured at 1.0σ, computed from a model in which substrate, drawn in red, is included. This drawing was generated using TURBO−FRODO (21).

Table 3: Refinement Statistics

final model	area detector data refinement (2.4 Å resolution)	synchrotron data refinement (1.9 Å resolution)
R-factor[a] (overall)	0.180	0.183
R-factor[a] (2.0−1.9 Å shell)		0.307
R-free	0.241	0.209
total residues	1280	1256
total non-H protein atoms	9962	9717
total PQQ molecules	2	2
total substrate molecules	2	2
total Ca^{2+} ions	2	2
total solvent molecules	0	612
RMSD[b] bond length (Å)	0.038	0.016
RMSD[b] bond angle (deg)	2.97	1.523
RMSD[b] dihedral angles (deg)	29.04	27.594
RMSD[b] improper angles (deg)	4.70	2.565
main chain *B*-factors (average/rms[c])	9	22/2.0
side chain *B*-factors (average/rms[c])	10	25/3.5
solvent *B*-factors (average)		29

[a] $R = \sum||F_o| - |F_c||/\sum|F_o|$, where F_o and F_c are the observed and calculated structure factor amplitudes. [b] Root-mean-square (rms) deviation from ideality. [c] The rms difference in *B*-factors for bonded atoms.

both subunits did not significantly move or become distorted during the refinement. Figure 2b shows the resulting electron density at this site in subunit H1, computed using coefficients $(2F_o - F_c)_{hkl}$ in the Fourier summation; the density in H2 is very similar to it. The corresponding ($F_o - F_c$) difference electron density map is featureless at this site in both subunits.

The second stage of crystallographic refinement utilized the 1.9 Å resolution synchrotron data and started with the model obtained using the multiwire data prior to the fitting of methanol. Refinement of positions and temperature factors, initially at 2.4 Å resolution, gave an *R*-factor of 0.196. The resolution was gradually extended to 2.0 Å with further positional and temperature factor refinement. Manual model rebuilding and water fitting were then carried out using ($2F_o - F_c$) and ($F_o - F_c$) difference electron density maps; the model was further refined and then extended to 1.9 Å resolution.

Up to this point, PQQ had been restrained so that the two carbonyl groups were coplanar with the ring system. However, with the synchrotron data, the PQQ showed significant nonplanar geometry after refinement, despite these restraints. The C5 protruded upward[2] toward the Cys103-Cys104 disulfide, and the O5 atom projected sharply downward, consistent with tetrahedral geometry at C5. C4, on the other hand, remained in the PQQ plane or slightly below it, and showed trigonal geometry, with its O4 atom

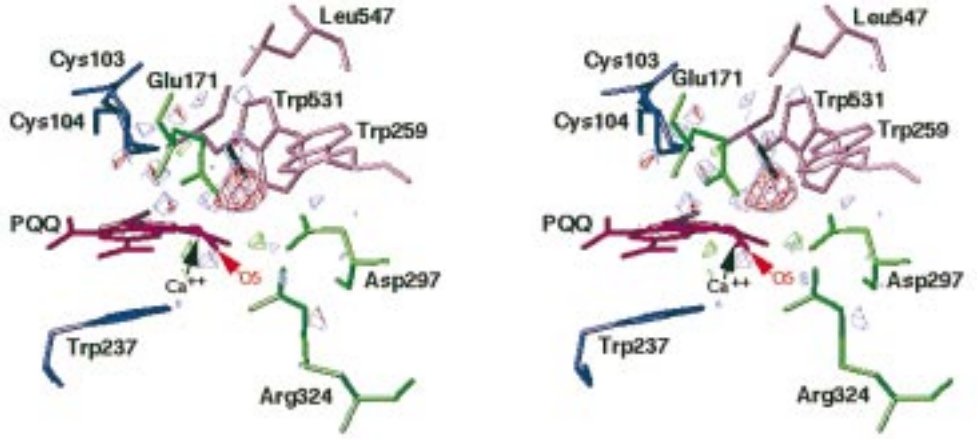

FIGURE 3: Simulated annealing "omit" difference electron density computed from a model in which substrate is not included, using the synchrotron data at 1.9 Å resolution and based on the model with tetrahedral restraints at C5 for PQQ. The map is contoured at $+3.0\sigma$ (in red), $+2.5\sigma$ (in light violet), and -3.0σ (in green). The surroundings of the substrate binding site are also shown. The black bond represents the methanol omitted from the model, with the methyl or methylene group and the hydroxyl group in the small top part and the large bottom part, respectively, of the ellipsoidal ($F_o - F_c$) electron density. This drawing was generated using TURBO−FRODO (*21*).

extending somewhat farther downward from the plane as a result of the tetrahedral geometry at C5. The ($2F_o - F_c$) electron density also agreed with this geometry, and the ($F_o - F_c$) electron density map contoured at $\pm 3.0\sigma$ showed positive electron density just above C5. A simulated annealing "omit" map (*22*), which was calculated by omitting PQQ and Ca^{2+} from the model and then slow-cooling from 1000 to 300 K, confirmed this result.

To determine the detailed configuration of PQQ, a variety of different test restraints was applied to C4 and C5 of PQQ and difference maps were examined after refinement in each case. Using trigonal and tetrahedral restraints in further refinement for C4 and C5, respectively, the PQQ behaved well in both subunits, and the resulting ($2F_o - F_c$) electron density agreed well with the model. The ($F_o - F_c$) electron density difference map is also featureless at the PQQ site. However, at the methanol site the ($F_o - F_c$) map contained positive ellipsoidal electron density similar to that assigned to methanol in the analysis of the multiwire data. Further refinement with methanol included in the model yielded featureless ($F_o - F_c$) difference density at this site. However, the ($2F_o - F_c$) electron density, especially at the methyl carbon, is significantly weaker than that from the multiwire data. Ellipsoidal, positive electron density from a simulated annealing "omit" map computed in the absence of methanol is shown in Figure 3.

The structure was further refined at 1.9 Å, and water with temperature factors higher than 50 Å^2 or in poor electron density was discarded. The C-terminal segments Ala58-Lys69 in both L subunits showed very poor electron density and very high temperature factors, indicating that they are disordered; they have been omitted from the final model.

Quality of the Model. The final model of the form *B* crystal structure of MEDH from *M.* W3A1, refined at 1.9 Å resolution, contains one H_2L_2 tetramer and 612 water molecules in an asymmetric unit. Each H subunit consists of 571 amino acid residues, one PQQ, one Ca^{2+}, and one molecule of substrate. Only 57 residues of each L subunit are included in the model, the 12 remaining C-terminal residues being disordered. Two different views of the PQQ model, refined at 1.9 Å resolution and superimposed on the ($2F_o - F_c$) electron density, are shown in Figure 4. In the Ramachandran plot (*23*) (not shown) the ϕ, ψ conformational angles of all nonglycine and nonproline residues, with one exception, are in the most favored and additionally allowed regions (*24*). Only in the case of Asp105 in both subunits do ϕ, ψ deviate from ideal values, because of strain from the unusual Cys103-Cys104 vicinal disulfide (*2*). The overall *R*-factor is 0.183 ($R_{free} = 0.209$), and the rms deviations of bond lengths and bond angles from ideal values are 0.016 Å and 1.5°, respectively. The refinement statistics are summarized in Table 3 and the average temperature factors of PQQ, Ca^{2+}, and methanol are shown in Table 4.

Structure of the Form B Crystals. As in the form *A* crystals, the polypeptide chain of each H subunit forms an 8-fold β-propeller superbarrel (Figure 5). Each L subunit lies across the surface of the H subunit and contains a long α-helix near the C-terminus. The C-terminal helices in both L subunits exhibit high temperature factors, which exceed 50 Å^2 for segment Arg54-Asn57 in subunit L1and for Lys53-Asn57 in L2. The complete disorder of the 12 remaining C-terminal residues in both L subunits indicates that these segments are more flexible in the form *B* crystals than in the form *A* crystals. Alternatively, proteolytic cleavage may have taken place during purification or crystallization of the enzyme.

The two HL dimers are related to each other by a noncrystallographic 2-fold symmetry axis approximately parallel to the crystallographic b axis. Together they form the H_2L_2 tetramer. The rms deviation of 628 Cα atoms between the two HL dimers of crystal form *B* is 0.15 Å, and that between crystal forms *A* and *B* is 0.24 Å. Some surface loops, such as Val311-Lys314, show obvious differences in conformation between the two dimers and between the two crystal forms. Some side chains on the molecular surface also differ between the two HL dimers; for example, the side chain of Ser35 in subunit H2 forms a hydrogen bond to the side chain of Asn33 in the same subunit, while in subunit H1 this serine forms a hydrogen bond to the carboxyl group of the side chain of Asp33 in subunit L1 of an adjacent molecule.

The active site structures in the two different crystal forms are basically the same. PQQ is located in a funnel-shaped

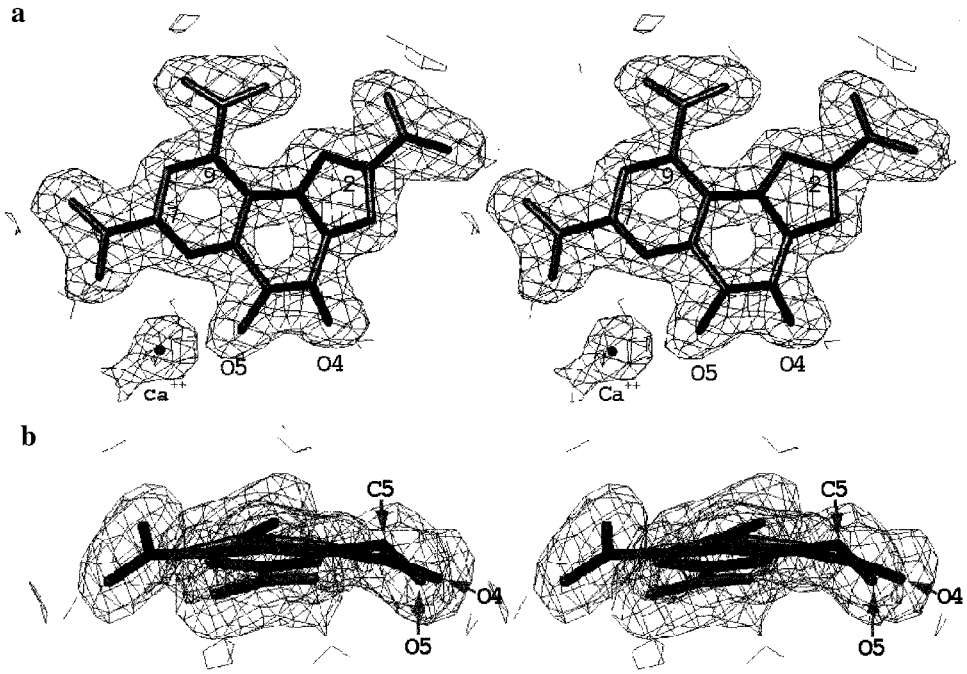

FIGURE 4: ($2F_o - F_c$) electron density showing the configuration of PQQ, computed using the synchrotron data at 1.9 Å resolution and based on the model with tetrahedral restraints at C5 for PQQ. The map is contoured at 1.0σ: (a) top view of the molecule; (b) end on view of the molecule. This drawing was generated using TURBO−FRODO (21).

Table 4: Temperature Factors (Å^2) of PQQ, Ca^{2+}, and Methanol

	area detector data (refined model)		synchrotron data (refined model)	
atom	subunit H1	subunit H2	subunit H1	subunit H2
PQQ	6−17	10−28	15−24	18−28
Ca^{2+}	9	6	43	42
CM1[a]	40	46	61	51
OM1[b]	39	47	56	48

[a] Methyl carbon atom of methanol. [b] Hydroxyl oxygen atom of methanol.

central channel, approximately on the pseudo 8-fold axis of the superbarrel, and it is sandwiched between the indole ring of Trp237 and the vicinal disulfide formed by residues Cys103 and Cys104. Ca^{2+} is hexacoordinate, with three of its six ligands coming from PQQ (atoms O5, N6, and O7a, see Figure 1) and the remaining three from protein side chain atoms Glu171 OE1, Glu171 OE2, and Asn255 OD1 (Figure 2). While both C4 and C5 of PQQ are in a planar configuration in the form *A* crystal structure (determined at 2.4 Å resolution), the structure of the form *B* crystals refined at 1.9 Å resolution shows a more complex configuration for PQQ, that is, C4 of PQQ is trigonal while C5 is tetrahedral, the average bond angle at the C5 and C4 atoms being 120° and 110°, respectively. As a result, C5 protrudes upward out of the mean PQQ plane forcing O5 to deviate downward, leading to a downward inclination of the plane containing C4, C5, C3a, and O4 (see Figure 1)

DISCUSSION

Substrate Binding. The substrate binding site was originally proposed to be close to O5 of PQQ (*25*). In the crystal structure of form *A* MEDH from *M.* W3A1, a water molecule makes a hydrogen bond to both O5 of PQQ and the side chain of Asp297 (*2*); its electron density is spherical, typical of a water molecule. In the form *B* crystal structure described here, the elongated electron density obtained from the multiwire data is consistent with the binding of a diatomic molecule at this site instead of the water. The nature of this ligand is not known with certainty, but is most likely methanol rather than formaldehyde. When isolated, MEDH is in the reduced or semiquinone form, depending on the isolation procedure (*26*). It is unable to react with substrate to give the product in the absence of a one-electron acceptor and does not react with dioxygen.

In the model refined using the synchrotron data, the hydroxyl of methanol appears to be hydrogen bonded to the side chain of Asp297 (at 3.1 Å), but not to the O5 of PQQ (at 3.4 Å) (Figure 6). The methyl group is surrounded by the hydrophobic side chains of Trp259, Trp531, and Leu547 as well as the vicinal disulfide. The high temperature factors of the two atoms of methanol resulting from the high-resolution refinement of the synchrotron data, listed in Table 4, indicate a low occupancy or high flexibility of the substrate.

The difference in the occupancy of methanol between the multiwire and synchrotron data sets, both recorded from *B*-form crystals grown from 4 mM methanol, may result from differences in crystal mounting. The two crystals used for synchrotron data collection were both mounted dry in sealed capillaries while the crystals used for the multiwire data collection were mounted wet in ~10 mM methanol-containing mother liquor. The methanol in the dry-mounted crystals may have partially evaporated and/or diffused elsewhere in the capillary. For the *A*-form crystals, where no methanol binding was observed (*2*), the artificial mother liquor used for wet mounting contained no methanol.

Mechanism. Two mechanisms have been proposed for the reaction catalyzed by MEDH (summarized in ref *1*). One mechanism involves the addition of methanol to PQQ to form a covalent hemiketal intermediate followed by elimination of formaldehyde (Figure 7). The other involves direct hydride

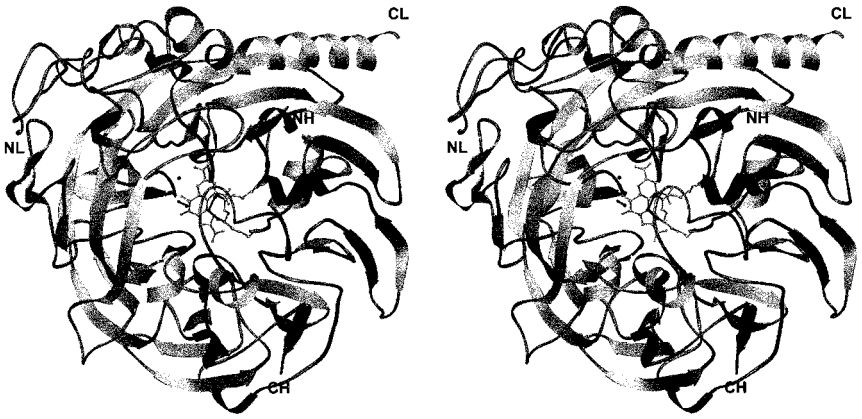

FIGURE 5: Stereo ribbon drawing of the heterodimer component of methanol dehydrogenase. The N and C termini of the H and L subunits are indicated. The PQQ prosthetic group is shown in gray ball-and-stick representation, and the methanol substrate and the calcium ion are shown in black. Above the PQQ is shown the side chain disulfide bridge of Cys103-Cys104 in black and its main chain atoms, and those of its adjacent residues, in gray. This drawing was made using RIBBONS (*30*).

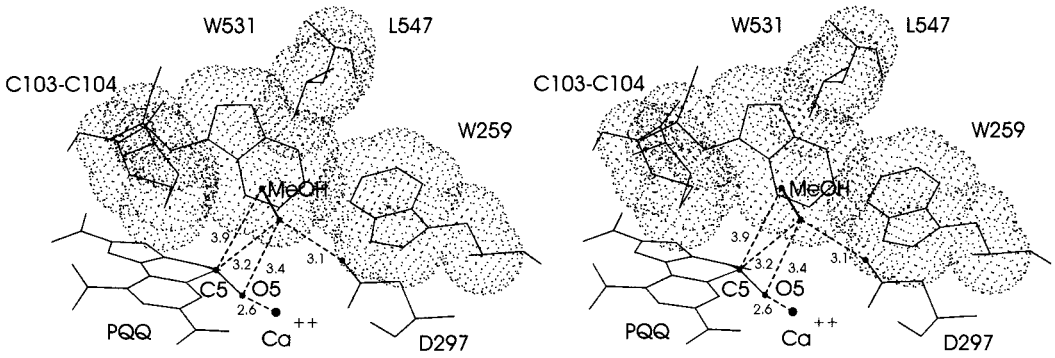

FIGURE 6: Protein environment of the substrate methanol in the form *B* crystals of methanol dehydrogenase from *M.* W3A1. The methyl group of methanol is above the hydroxyl group which is hydrogen bonded to Asp297. Distances shown are in angstroms. The coordination bond between O5 and Ca^{2+} is also shown. This drawing was generated using TURBO−FRODO (*21*).

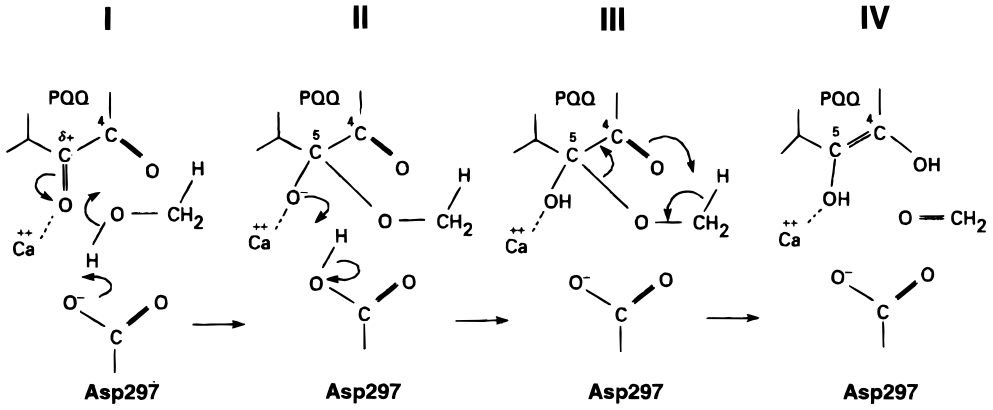

FIGURE 7: Addition−elimination mechanism for oxidation of methanol by PQQ in methanol dehydrogenase (after Anthony et al., 1994 (*1*)). I represents methanol bound to the resting enzyme. II represents the hemiketal intermediate after proton abstraction by Asp297 from the substrate hydroxyl and attack of the resulting oxyanion on C5. III represents reduction of PQQ and transfer of a proton from the substrate methyl to O4 of PQQ followed in IV by release of the formaldehyde product.

transfer from methanol to PQQ. Both of these mechanisms require, as a first step, the deprotonation of the substrate hydroxyl by a catalytic base to initiate the reaction. The second step is then either creation of the hemiketal intermediate through formation of a carbon−oxygen bond at C5 or transfer of the hydride ion from the substrate methyl group to the C5 atom. Experimental evidence supporting the addition−elimination mechanism is provided by the fact that C5 of free PQQ can readily form adducts with methanol and other small molecules (*27*). Furthermore, Itoh et al. (*28*) showed that hemiacetal adducts could be isolated from a solution of the trimethyl ester of PQQ in methanol, and reported that the crystal structure of one of the adducts showed methanol bound to the C5 atom.

In the active site, Asp 279 is well situated to serve as the catalytic base in the first step of abstracting a proton from the hydroxyl oxygen of methanol, since one of its carboxylates is 3.1 Å from the hydroxyl oxygen (Figure 6). The orientation of the methanol in the active site lends further support to the hemiketal mechanism (Figure 7). The hydroxyl oxygen is close to C5 (3.2 Å) while the methyl group is considerably farther away (3.9 Å). This would favor covalent

bond formation between C5 and the nearby hydroxyl over hydride ion transfer from the more distant methyl group of the substrate.

Nature of the Tetrahedral Configuration at C5 of PQQ. One possible explanation for C5 being tetrahedral in the form *B* crystals is that adduct formation has taken place. Free oxidized PQQ will form adducts with water and with ammonia at the C5 position making the carbon tetrahedral (*27*). However, since PQQ bound to MEDH is in the reduced or semiquinone state when isolated (*26*), it is not known if adduct formation could occur. To test this possibility, the PQQ was modeled as the C5-methanol adduct and refined. This led to strong disagreement between the model and the resulting ($2F_o - F_c$) electron density map and produced strong negative ($F_o - F_c$) electron density at the bound methanol position, thereby ruling out the possible existence of a C5 adduct in the crystal structure.

If the PQQ is fully reduced, the planar form of the prosthetic group is likely to predominate, stabilized by delocalization of the electrons in the aromatic ring and both the C4 and C5 atoms would be trigonal.[4] If the PQQ is in the semiquinone state, it could exist in two tautomeric forms in which either of the two quinone oxygens is in the hydroxyl form. The two forms would be energetically equivalent except for perturbations caused by the protein environment. Each tautomer can be drawn in two resonance forms, one with the unpaired electron delocalized on the ring and the other with the electron localized to the quinone oxygen. The presence of Ca^{2+}, 2.6 Å from O5 (Figure 6), might stabilize the negatively charged quinone oxygen and permit distortion of C5 to a tetrahedral geometry.

In the crystal structure of MEDH from *M. extorquens* AM1, determined at 1.94 Å resolution (*7*), PQQ was also found to be distorted. In this case, however, O4 projected sharply downward from the PQQ plane while O5 remained in the plane. No distortion of the C4 or C5 atom from trigonal to tetrahedral geometry was reported. Also, no diatomic molecule appeared to be present in the active site, indicating that substrate and product were not present or were not well ordered. The explanation presented for the observed geometry was that PQQ was trapped in a semiquinone state. Thus, the tautomeric states of PQQ in the proteins from the two bacterial systems appear to be quite different. The crystallization conditions of the two proteins are similar; however, the presence or absence of methanol during crystallization or data collection of the MEDH from *M. extorquens* AM1 was not discussed (*7*).

ACKNOWLEDGMENT

We wish to thank Prof. N. Sakabe, Dr. H. Watanabe, Dr. Ikemizu, and Mr. Sasaki for their help with the synchrotron data collection. We also wish to thank Drs. H. Duine and V. L. Davidson for helpful suggestions.

[4] A possible tautomeric form of reduced PQQ in which a proton, on the pyrrole nitrogen atom N1, migrates to C5 and the bonds of the indole ring redistribute to stabilize a tetrahedral configuration at C5 seems unlikely since the proton at N1 is involved in a strong intramolecular hydrogen bond (2.6 Å) with the carboxylate oxygen O9B, as observed in the present MEDH structure and in the structure of PQQ itself (*3, 28*).

REFERENCES

1. Anthony, C., Ghosh, M., and Blake, C. C. F. (1994) *Biochem. J. 304*, 665−674.
2. Xia, Z.-x., Dai, W.-w., Zhang, Y.-f., White, S. A., Boyd, G. D.,and Mathews, F. S. (1996) *J. Mol. Biol. 259*, 480−501.
3. Salisbury, S. A., Forrest, H. S., Cruse, W. B. T., andKennard, O. (1979) *Nature 280*, 843−844.
4. Richardson, I. W., and Anthony, C. (1992) *Biochem. J. 287*, 709−715.
5. Xia, Z.-x., Dai, W.-w., Xiong, J.-p., Hao, Z.-p., Davidson, V. L., White, S. A., and Mathews, F. S. (1992) *J. Biol. Chem. 267*, 22290−22297.
6. White, S. A., Boyd, G., Mathews, F. S., Xia, X.-x., Dai, W.-w., Zhang, Y.-f., and Davidson, V. L. (1993) *Biochemistry 32*, 12955−12958.
7. Ghosh, M., Anthony, C., Harlos, K., Goodwin, M. G., and Blake, C. (1995) *Structure 3*, 177−187.
8. Rossman, M. G. (1972) in *The Molecular Replacement Method* (Rossman, M. G., Ed.) pp 4−15, Gorden & Breach, New York.
9. Kasprzak, A. A., and Steenkamp, D. J. (1983) *J. Bacteriol. 156*, 348−353.
10. Xia, Z.-x., Hao, Z.-p., Mathews, F. S., and Davidson, V. L. (1989) *FEBS Lett. 258*, 175−176.
11. Matthews, B. W. (1968) *J. Mol. Biol. 33*, 491−497.
12. Howard, A. J., Nielsen, C., and Xuong Ng., H. (1985) *Methods Enzymol. 114*, 452−472.
13. Sakabe, N. (1983) *J. Appl. Crystallogr. 16*, 542−547.
14. Otwinowski, Z., and Minor, W. (1997) *Methods Enzymol. 276*, 307−326.
15. Fitzgerald, P. M. D. (1988) *J. Appl. Crystallogr. 21*, 273−278.
16. Crowther, R. A. (1972) in *The Molecular Replacement Method* (Rossman, M. G., Ed.) pp 173−178, Gorden & Breach, New York.
17. Lattman, E. E., and Love, W. E. (1970) *Acta Crystallogr., Sect. B 26*, 1854−1857.
18. Crowther, R. A., and Blow, D. M. (1967) *Acta Crystallogr. 23*, 544−548.
19. Hendrickson, W. A. (1985) *Methods Enzymol. 115*, 252−270.
20. Brunger, A. T. (1993) X-PLOR (version 3.1) *Manual of a system for crystallography and NMR*, Yale University, New Haven, CT.
21. Roussel, A., and Cambillau, C. (1991) TURBO−FRODO, in *Silicon Graphics Geometry Partners Directory* 86, Silicon Graphics, Moutain View, CA.
22. Hodel, A., Kim, S.-H., and Brunger, A. T. (1992) *Acta Crystallogr., Sect. A 48*, 851−858.
23. Ramachandran, N., and Sasisekharan, V. (1968) *Adv. Protein Chem. 28*, 283−437.
24. Laskowski, R. A., MacArthur, M. W., Moss, D. S., and Thornton, J. M. (1993) *J. Appl. Crystallogr. 26*, 283−291.
25. Duine, J. A., Frank, J., and Jongejan, J. A. (1987) *Adv. Enzymol. 59*, 169−212.
26. Anthony, C. (1996) *Biochem. J. 320*, 697−711.
27. Dekker, R. H., Duine, J. A., Frank, J., Verwiel, P., and Westerling, J. (1982) *Eur. J. Biochem. 125*, 69−73.
28. Itoh, S., Ogino, M., Fukui, Y., Murao, H., Komatsu, M., Ohshiro, Y., Inoue, T., Kai, Y., and Kasai, N. (1993) *J. Am. Chem. Soc. 115*, 9960−9967.
29. Ishida, T., Doi, M., Tomita, K., Hayashi, H., Inoue, M., and Urakami, T. (1989) *J. Am. Chem. Soc. 111*, 6822−6828.
30. Carson, M. (1997) *Methods Enzymol. 277*, 493−505.

BI9822574